Dysfunction of oskyddad causes harlequin-type ichthyosis-like defects in Drosophila Melanogaster

Yiwen Wang, Michaela Norum, Kathrin Oehl, Yang Yang, Renata Zuber, Jing Yang, Jean-Pierre Farine, Nicole Gehring, Matthias Flötenmeyer, Jean-François Ferveur, et al.

PLOS GENETICS

RESEARCH ARTICLE

Dysfunction of Oskyddad causes Harlequin-type ichthyosis-like defects in *Drosophila melanogaster*

Yiwen Wang[1,2☯], Michaela Norum[1☯], Kathrin Oehl[1], Yang Yang[1], Renata Zuber[1,3], Jing Yang[1], Jean-Pierre Farine[4], Nicole Gehring[1], Matthias Flötenmeyer[5], Jean-François Ferveur[4], Bernard Moussian[1,6]*

1 Section Animal Genetics, Interfaculty Institute of Cell Biology, University of Tübingen, Tübingen, Germany, **2** School of Pharmaceutical Science and Technology, Tianjin University, Tianjin, China, **3** Applied Zoology, Technical University of Dresden, Dresden, Germany, **4** Centre des Sciences du Goût et de l'Alimentation, UMR-CNRS 6265, Université de Bourgogne, Dijon, France, **5** Microscopy Unit, Max-Planck-Institut für Entwicklungsbiologie, Tübingen, Germany, **6** Institute of Biology Valrose, CNRS, Inserm, Université Côte d'Azur, Nice, France

☯ These authors contributed equally to this work.
* bernard.moussian@unice.fr

OPEN ACCESS

Citation: Wang Y, Norum M, Oehl K, Yang Y, Zuber R, Yang J, et al. (2020) Dysfunction of Oskyddad causes Harlequin-type ichthyosis-like defects in *Drosophila melanogaster*. PLoS Genet 16(1): e1008363. https://doi.org/10.1371/journal.pgen.1008363

Editor: David L. Stern, Janelia Farm Research Campus, Howard Hughes Medical Institute, UNITED STATES

Received: August 8, 2019

Accepted: December 17, 2019

Published: January 13, 2020

Data Availability Statement: All relevant data are within the manuscript and its Supporting Information files.

Funding: This work was supported by a grant to BM by the German Research Foundation (DFG, MO1714/9-1) and a grant to YY by the National Science Foundation of China (NSFC, 31761133021). The funders had no role in study design, data collection and analysis, decision to publish, or preparation of the manuscript.

Abstract

Prevention of desiccation is a constant challenge for terrestrial organisms. Land insects have an extracellular coat, the cuticle, that plays a major role in protection against exaggerated water loss. Here, we report that the ABC transporter Oskyddad (Osy)—a human ABCA12 paralog—contributes to the waterproof barrier function of the cuticle in the fruit fly *Drosophila melanogaster*. We show that the reduction or elimination of Osy function provokes rapid desiccation. Osy is also involved in defining the inward barrier against xenobiotics penetration. Consistently, the amounts of cuticular hydrocarbons that are involved in cuticle impermeability decrease markedly when Osy activity is reduced. GFP-tagged Osy localises to membrane nano-protrusions within the cuticle, likely pore canals. This suggests that Osy is mediating the transport of cuticular hydrocarbons (CHC) through the pore canals to the cuticle surface. The envelope, which is the outermost cuticle layer constituting the main barrier, is unaffected in *osy* mutant larvae. This contrasts with the function of Snu, another ABC transporter needed for the construction of the cuticular inward and outward barriers, that nevertheless is implicated in CHC deposition. Hence, Osy and Snu have overlapping and independent roles to establish cuticular resistance against transpiration and xenobiotic penetration. The *osy* deficient phenotype parallels the phenotype of Harlequin ichthyosis caused by mutations in the human *abca12* gene. Thus, it seems that the cellular and molecular mechanisms of lipid barrier assembly in the skin are conserved during evolution.

Competing interests: The authors have declared that no competing interests exist.

Author summary

As in humans, lipids on the surface of the skin of insects protect the organism against excessive water loss and penetration of potentially harmful substances. During evolution, a greasy surface was indeed an essential trait for adaptation to life outside a watery environment. Here, we show that the membrane-gate transporter Oskyddad (Osy) is needed for the deposition of barrier lipids on the integument surface in the fruit fly *Drosophila melanogaster* through extracellular nano-tubes, called pore canals. In principle, the involvement of Osy parallels the scenario in humans, where the membrane-gate transporter ABCA12 is implicated in the construction of the lipid-based stratum corneum of the skin. In both cases, mutations in the genes coding for the respective transporter cause rapid water-loss and are lethal soon after birth. We conclude that the interaction between the organism and the environment obviously implies an analogous mechanism of barrier formation and function in vertebrates and invertebrates.

Introduction

To avoid desiccation, animals build a lipid-based barrier on their outer surface. In mammals, the stratum corneum, which is the uppermost skin layer, consists of corneocytes and a composite lipid-rich matrix including ceramides that are either free or bound to so-called cornified envelope proteins [1]. A number of ceramide-producing and transporting enzymes have been identified to participate in the formation of the lipid matrix [2, 3]. A key player in this process is the ATP-binding cassette transporter A12 (ABCA12) that loads ceramides into specialized secretory vesicles the so-called lamellar granules before they are deposited into the extracellular space. ABCA12 dysfunction through mutations in the respective gene leads to the failure to form the ceramide matrix, thereby causing different types of congenital ichthyosis that are associated with excessive transepidermal water loss, impaired thermoregulation and enhanced infection sensitivity in mice and humans [4–10]. In severe cases, *ABCA12* mutations may be lethal to the neonate (https://www.omim.org/entry/242500).

Like vertebrates, insects are covered by a protective stratified extracellular matrix (ECM) consisting of the innermost chitinous procuticle, the upper protein-lipid epicuticle and the outermost envelope produced by the underlying epidermis [11]. The envelope constitutes the first water- and xenobiotics-repellent barrier and is mainly composed of free and bound lipids [12]. Biosynthesis of these lipid compounds involves enzymes acting especially in oenocytes that form clusters underneath the epidermis [13, 14]. In the fruit fly *Drosophila melanogaster*, cuticular hydrocarbon (CHC) production in oenocytes, indeed, is sufficient to protect the animal against desiccation [15]. While some of the molecules and responsible genes involved have been identified [16], the molecular and cellular mechanisms of the lipid-based barrier organisation are not well understood.

Recently, we identified and characterised the function of the ABC transporter Snustorr (Snu) in constructing an inward and outward barrier in the *D. melanogaster* cuticle [17]. In *D. melanogaster*, Snu is needed for correct localisation of the extracellular protein Snustorr-snarlik (Snsl) at the tips of the pore canals that serve as routes for lipid transport through the procuticle. In *snu* mutant larvae, the envelope is incomplete causing rapid water loss and larval death. Moreover, the cuticle of these animals is permeable to xenobiotics indicating that Snu activity is required for the construction of both the outward and inward barrier. The function of Snu is evolutionary conserved given that its homolog LmABCH-9C in the migratory locust *Locusta migratoria* is necessary to build the cuticular desiccation barrier [18]. Consistently, in

the red flour beetle *Tribolium castaneum*, the putative Snu orthologue TcABCH-9C has been reported to control the amounts of cuticle lipids [19].

With a single ATPase and a single transmembrane domain, Snu and its putative orthologues are, in contrast to the full ABCA12 transporter, half-type ABC transporters, that need dimerisation with other half-type transporters in order to be active: they either form homo- or heterodimers. Thus, Snu possibly needs a partner ABC transporter for proper function. The genome of many insects also harbours two other genes coding for H-type ABC transporters, ABCH-9A and ABCH-9B [18–23] that may be candidate Snu partners (S1 Fig). While insects have three ABCH transporters, other arthropods such as crustaceans and arachnids have multiple copies of this class of transporters [24]. According to phylogenetic analyses, the common ancestor of insects and crustacean had one ABCH type transporter: CG11147/LmABCH-9A, which is likely the primary ancestral protein of this transporter family in insects. The CG11147 coding gene is expressed in the digestive tract during embryogenesis and is therefore unlikely to be required for cuticle formation. The ABCH-9B coding gene, by contrast, is expressed in the embryonic epidermis that produced the larval cuticle. Here, we have focussed our study on the function of ABCH-9B transporters during cuticle differentiation in *D. melanogaster*.

Results

CG33970 codes for a ABCH-type transporter related to the human ABCA transporters

In our RNAi-based screen for genes needed for larval cuticle formation [17], we discovered a candidate gene (*CG33970*) affecting larval resistance to desiccation. Prior to functional characterisation of CG33970, we examined the organisation of the corresponding locus. According to flybase (flybase.org), the *CG33970* locus gives rise to three alternative transcripts including two long transcripts (A and B) and one short transcript (C) (Fig 1). The transcript C yields a short protein, which lacks the 287 N-terminal amino acids of the proteins encoded by the transcripts A and B. Since these two transcripts differ only in non-coding regions, they produce identical full-length proteins. The respective protein sequence has 777 residues with an ATPase domain in the N-terminal half of the protein (also called nucleotide-binding domain, NBD) and a domain with six transmembrane helices (ABC2 domain) in the C-terminal half of the protein. Thus, CG33970 belongs to the group of half-type ATP-binding cassette (ABC) transporters [25]. Using specific primers, we confirmed the expression of the predicted long and the short transcripts by qPCR.

To learn about the potential molecular function of CG33790, using the full-length CG33790 protein, we searched the NCBI database for human homologous sequences that have been functionally characterised. The most homologous sequences were ABCA-type transporters including ABCA3 and ABCA12 (Fig 1). ABCA-type transporters are full transporters that are mainly involved in lipid transport across membranes [26]. Hence, it is possible that CG33790 is implicated in lipid transport in *D. melanogaster*.

Knock-down of CG33970/osy causes immediate post-embryonic desiccation

To investigate the function of the ABC transporter CG33970, we suppressed the expression of all transcripts either in the epidermis or ubiquitously by targeting the UAS-driven transcription of the hairpin RNAs (hpRNA) GD297 (Fig 1) either with *69B*-Gal4 (Fig 2) or with the *da/7063*-Gal4 drivers, respectively. These larvae became slack just after hatching and they died (see below). Larvae ubiquitously expressing the hpRNA KK109988 that is directed against the

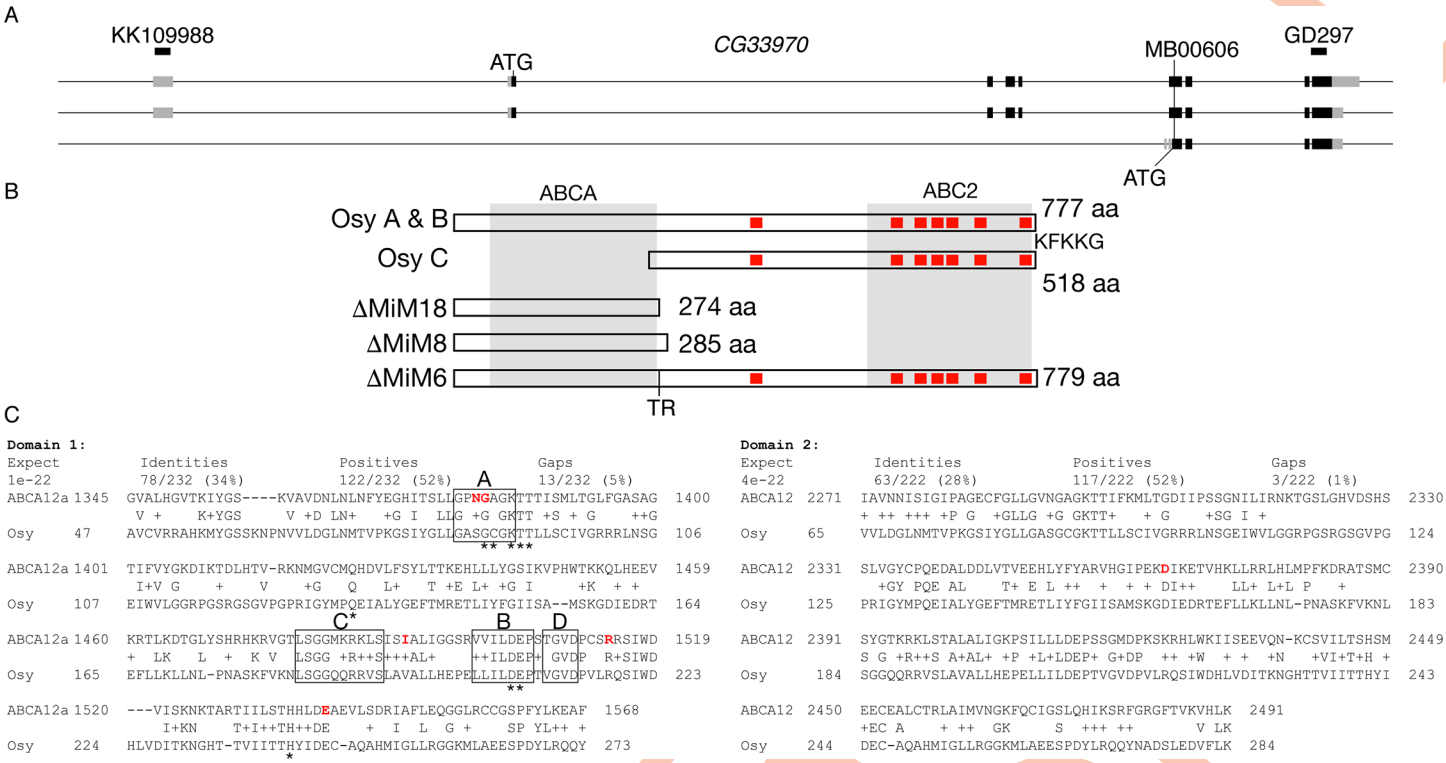

Fig 1. Osy is a half-type ABC transporter. The *CG33970/osy* locus yields three types of transcripts (A), two long and one short mRNAs. The long transcripts are both translated to a 777 residues containing protein with an ABCH domain in its N-terminal half (amino acids 48–270), and an ABC2 domain (amino acids 394–770) containing six transmembrane domains (red boxes) in its C-terminal half (B). Based on this composition, Osy can be assigned to the class of half-type ABC transporters. In addition, the last five amino acids of the protein (KFKKG) constitute an ER-retention signal. The transposon MB00606 in the 8th exon was excised to obtain alleles coding for dysfunctional proteins. Three lethal excision alleles were sequenced, ΔMiM18, ΔMiM8 and ΔMiM6. These three alleles have insertions of 4 (ΔMiM18), 8 (ΔMiM8) or 6 bp (ΔMiM6) at the position of transposon insertion (in codon number 273). The ΔMiM18 and ΔMiM8 insertions cause frame-shifts resulting in stop codons soon downstream of the insertion site in turn yielding proteins that are devoid of the ABC2 domain. Through the ΔMiM6 insertion, the protein gains two amino acids (TR) in the region linking the ABCH and the ABC2 domains. Alignment of the full-length Osy protein with human ABCA3 and ABCA12 (C). The sequence of the full length Osy protein was blasted against human proteins in the NCBI database using the BlastP software (https://blast.ncbi.nlm.nih.gov/). The Osy ABC cassette domain displays significant homology to both of the respective domains (domain 1 and 2) in all human ABCA transporters. Here, we show the alignment of these domains in ABCA3 and ABCA12 (isoform a). Those amino acids mutated on ABCA12 variants are highlighted in red (Akiyama, 2010). The respective amino acids are marked in orange in the ABCA3 sequence. Not all of these residues are conserved in this sequence.

https://doi.org/10.1371/journal.pgen.1008363.g001

long transcripts eventually hatched, but dried out and died about 11 minutes after hatching (Table 1). In general, larvae expressing hpRNA against *CG33970* did not show any obvious morphological defect (Fig 2). Addition of halocarbon oil to newly hatched *CG33970*$^{da/7063\text{-}IR}$ knockdown larvae rescued their lethality (Table 1). The drying-out phenotype prompted us to name *CG33970 oskyddad* (*osy*, Swedish for unprotected). In summary, lethality and loss of turgidity just after hatching were induced when hpRNAs against *osy* were expressed under the control of the epidermal *69B*-Gal4 or *da*/*7063*-Gal4 drivers.

Of note, the identical phenotypes caused by expression of KK109988 and GD297 suggests that a possible down-regulation of the potential KK109988 off-target *CG11147* (coding for ABCH-9A, predicted by VDRC) did not contribute to the phenotypes (see discussion).

Using the RNAi technique, we finally sought to address a possible function of Osy in the oenocytes. Indeed, due to a strong epidermal signal, the *in situ* hybridization data on Fly Express (http://www.flyexpress.net) cannot exclude an expression of *osy* (i.e. *CG33970*) in the oenocytes. Expression of hpRNA against *osy* in the oenocytes using a oenocyte-specific Gal4 (BO-Gal4 [13]) did not supress *osy* expression (S2 Fig) and was not lethal at any time of the *D.*

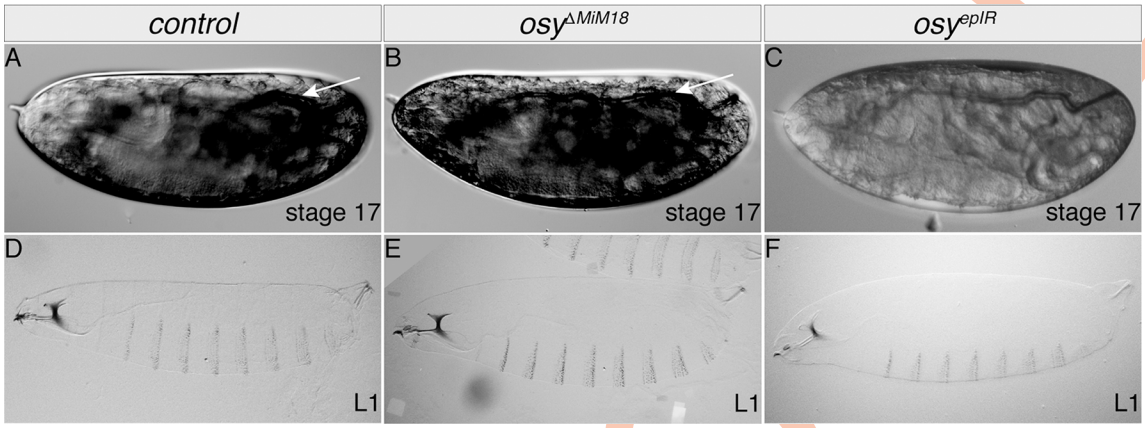

Fig 2. Mutations in the osy gene are lethal. Wild-type stage 17 embryos ready to hatch fill the egg space (A). They have gas-filled tracheae (arrow). Stage 17 embryos homozygous for the *osy* allele Δ*MiM18* (B) or expressing the hpRNA GD297 *osy* in the epidermis using *69B*-Gal4 (C, osy^{epIR}) appear to be normal. Like wild-type 1st instar larvae (D), *osy* mutant 1st instar larvae (E) and 1st instar larvae with reduced *osy* expression (F) hatch, but die soon thereafter (see also Table 1).

https://doi.org/10.1371/journal.pgen.1008363.g002

melanogaster lifecycle. This result indicates that even if *osy* was expressed in the oenocytes, its function in these cells is not essential.

To confirm the subtle phenotype caused by *osy* reduced expression, we generated stable *osy* mutant alleles by imprecise excision of the *Minos* transposon element *Mi00606* inserted into the exon 7 of the isoforms A and B common coding sequence (see materials & methods and Fig 1). The line segregating the frame shift mutation $osy^{\Delta MiM18}$ (Fig 1, additional 4bp, protein length 274 amino acids before a premature stop codon) was used for detailed phenotypic analyses in the following part of our study. Larvae homozygous for $osy^{\Delta MiM18}$ did not show any obvious morphological phenotype (Fig 2). Like the knock-down larvae described above, they hatched, immobilized, flattened and died (S3 Fig). Ubiquitous or epidermal expression of a C-terminally GFP-tagged version of the long isoform of Osy (Osy-GFP) in $osy^{\Delta MiM18}$ larvae using the UAS/Gal4 system (*69B*-Gal4 and *da/7063*-Gal4) rescued the viability and animals survived to adulthood. This result argues that the full-length Osy protein is sufficient for outward barrier construction in the *D. melanogaster* cuticle.

Penetration resistance depends on CG33970 function

The dehydration phenotype of larvae with down-regulated *osy* expression (osy^{epIR} and osy^{ubIR}) suggests an increased permeability of their cuticle. To test this hypothesis, we incubated these larvae in Eosin Y in a penetration assay [27, 28] (Fig 3). In these larvae, the reduced Osy function did not cause an abnormal Eosin Y uptake at room temperature (22˚C), whereas in *snu* mutant larvae Eosin Y penetrates the tissue in the same assay. At 40˚C, however, the cuticle of

Table 1. Osy function prevents desiccation.

treatment	wild-type	osy^{ubIR}
Survival time on agar plate	>2h (n = 13)	11min +/- 1.7 (n = 10)
Survival time on glass & oil	>2h (n = 11)	>2h (n = 11)

On agar plates, newly hatched wild-type larvae and larvae ubiquitously (using *da/7063*-Gal4) expressing hpRNA (KK109988) against *osy* (osy^{ubIR}) were observed for at least two hours (>2h). The second experiment was done on glass because the halocarbon oil would spread on an agar substrate exposing the larvae to the air.

https://doi.org/10.1371/journal.pgen.1008363.t001

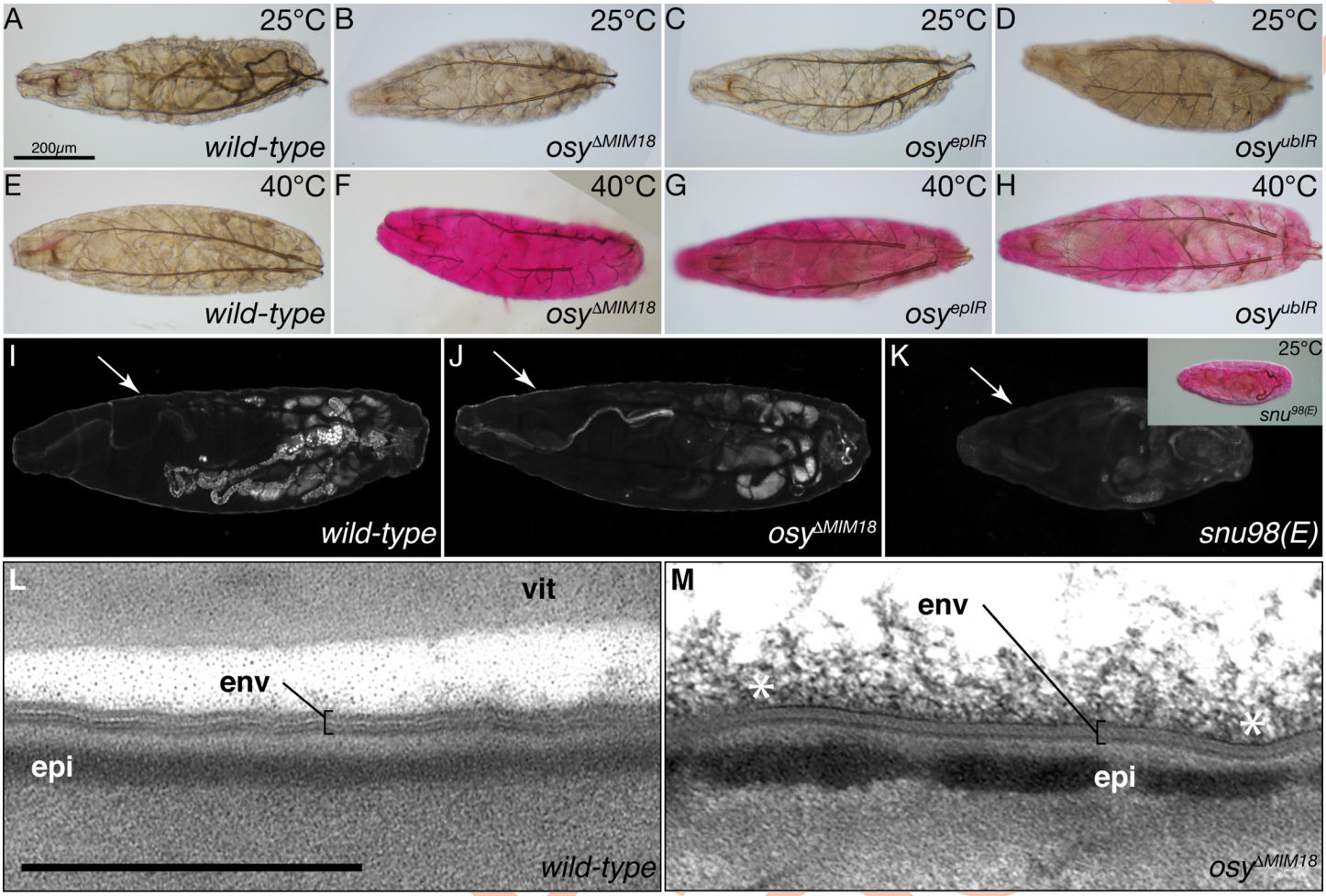

Fig 3. Osy function prevents penetration of xenobiotics. In dye penetration assays, the 1st instar wild-type (A) and *osy* mutant ($osy^{\Delta MiM18}$, B) larvae do not take up Eosin Y at 25˚C Down-regulation of *osy* transcripts by epidermal RNAi (osy^{epIR}, *69B*-Gal4 x UAS-KK109988, C) or ubiquitous (osy^{ubIR}, *da/7063*-Gal4 x UAS-KK109988, D) RNAi does not cause dye penetration at 25˚C in 1st instar larvae. At 40˚C, the cuticle of wild-type 1st instar larvae is impermeable to Eosin Y (D), while in *osy* mutant 1st instar larvae the dye penetrates the cuticle (E). At 25˚C, in 1st instar larvae with reduced *osy* transcript levels in the whole body (F) or in the epidermis (G), Eosin Y does not penetrate the cuticle. The cuticle of 1st instar larvae with reduced *osy* transcript levels in the whole body (H) or in the epidermis (I) fails to withstand dye penetration at 40˚C. The envelope (arrow) of the wild-type 1st instar larva auto-fluoresces upon excitation with UV light (I). Envelope auto-fluorescence is unchanged in $osy^{\Delta MiM18}$ 1st instar larvae (J). By contrast, envelope auto-fluorescence is reduced in *snu* mutant 1st instar larvae (K). This defect allows Eosin Y penetration into these larvae at 25˚C (inset). The envelope (env) of wild-type stage 17 ready-to-hatch embryos consists of alternating electron-lucid and electron-dense sheets in electron-micrographs (L). The envelope of stage 17 ready-to-hatch $osy^{\Delta MiM18}$ embryos is normal in electron-micrographs (M). The asterisks (*) mark unspecific material at the surface of the cuticle. vit vitelline membrane. Scale bar 500nm.

https://doi.org/10.1371/journal.pgen.1008363.g003

larvae with reduced *osy* expression was permeable to Eosin Y, while it was not in the wild-type cuticle tested under similar condition. Impermeability to Eosin Y was restored in $osy^{\Delta MiM18}$ larvae that ubiquitously expressed Osy-GFP (S4 Fig). This result indicates that the full-length Osy isoform is responsible for inward barrier function in *D. melanogaster*.

We also stained wings with Eosin Y to test whether RNAi-mediated suppression of *osy* expression affected cuticle permeability in this simple tissue (S5 Fig). Suppression of *osy* expression under the control of the wing specific driver *nub*-Gal4 caused penetration of Eosin Y at a non-permissive temperature. Taken together, these experiments suggest that the suppression of *osy* expression affects both the outward and the inward barrier.

The envelope of osy mutant larvae is normal

To explore the integrity of the envelope in larvae with reduced or eliminated Osy function, we analysed its auto-fluorescence property when excited with UV light by confocal microscopy [17]. The auto-fluorescence of the envelope in $osy^{\Delta MiM18}$ mutant larvae was similar to the signal in wild-type larvae, whereas it was markedly reduced in *snu* mutant larvae (Fig 3J–3L).

We next examined the potential consequences of Osy dysfunction in the cuticle by transmission electron microscopy of ultrathin sections (Fig 3M and 3N). The cuticle architecture of $osy^{\Delta MiM18}$ homozygous larvae appeared to be normal. Especially, the organisation of the envelope that constitutes a main waterproof barrier was unaffected. Therefore, we conclude that the overall structure of the envelope does not require Osy function.

Osy localises to the apical plasma membrane and probably to pore canals

In order to deepen our understanding on Osy function, we determined its sub-cellular localisation. We examined by confocal microscopy the distribution of a chimeric Osy protein with N-terminally fused GFP (GFP-Osy, a UAS-construct driven by *da*-Gal4/*7063*-Gal4) in live L3 larvae. GFP-Osy, which is able to restore cuticle impermeability in $osy^{\Delta MiM18}$ mutant larvae (S4 Fig, see above), localises to the apical plasma membrane of epidermal cells (Fig 4). Besides a faint uniform localisation at the cell surface, we observed bright GFP-Osy dots. These dots co-localise with dots formed by CD8-RFP (Fig 4), a membrane marker that also labels membrane protrusions within the cuticle, possibly pore canals [17].

To substantiate the possibility that GFP-Osy may be localised to putative pore canals, we co-expressed GFP-Osy (driven by *da*-Gal4/*7063*-Gal4) with Snsl-RFP that marks the tips of these membrane protrusions before they enter the epicuticle [17]. Most GFP-Osy marked dots are also positive for Snsl-RFP (Fig 4). Thus, we conclude that Osy is present in epidermal membrane protrusions that are required for cuticle barrier formation in the *D. melanogaster* larva.

Snu localises to the apical plasma membrane independently of Osy

Osy and Snu are both half-type ABC transporters with a C-terminal ER-retention signal [17]. This type of ER retention signal needs to be masked through protein-protein interaction in order that the protein can transfer to the Golgi and ultimately to the plasma membrane [29]. In order to test whether the localisation of Snu in the apical plasma membrane depends on Osy, we observed the distribution of Snu-GFP in $osy^{\Delta MiM18}$ mutant larvae (Fig 5). In wild-type control larvae and in $osy^{\Delta MiM18}$ mutant larvae, Snu-GFP localized to the apical plasma membrane of epithelial cells. Thus, functional Osy is not required for Snu localisation in the apical plasma membrane. This suggests that Osy and Snu do not interact to form a full ABC transporter.

Osy is required for CHC deposition at the surface of the wing cuticle

CHCs constitute a barrier on the cuticle surface. We quantified and compared their absolute and relative amounts on the wing surface of wild-type flies and flies with reduced *osy* expression after 6 hours post eclosion and at day 5 after eclosion (Fig 6, S6 Fig). When wing-specific RNAi-mediated suppression of *osy* or *snu* were targeted by the nub-Gal4 driver, the resulting wings showed a significant reduction of the total amount of CHCs at both ages compared to the wild type (Dijon 2000) and transgenic control (*nub*-Gal4 x UAS-*CS-2*-IR). Differently, the qualitative variation of the major CHCs types showed no relationship with wing-targeted suppression of *osy* or *snu* expression. Thus, Osy does not seem to have a specific type of substrate but is required for the quantitative deposition of all recorded CHCs on the surface of the wing cuticle.

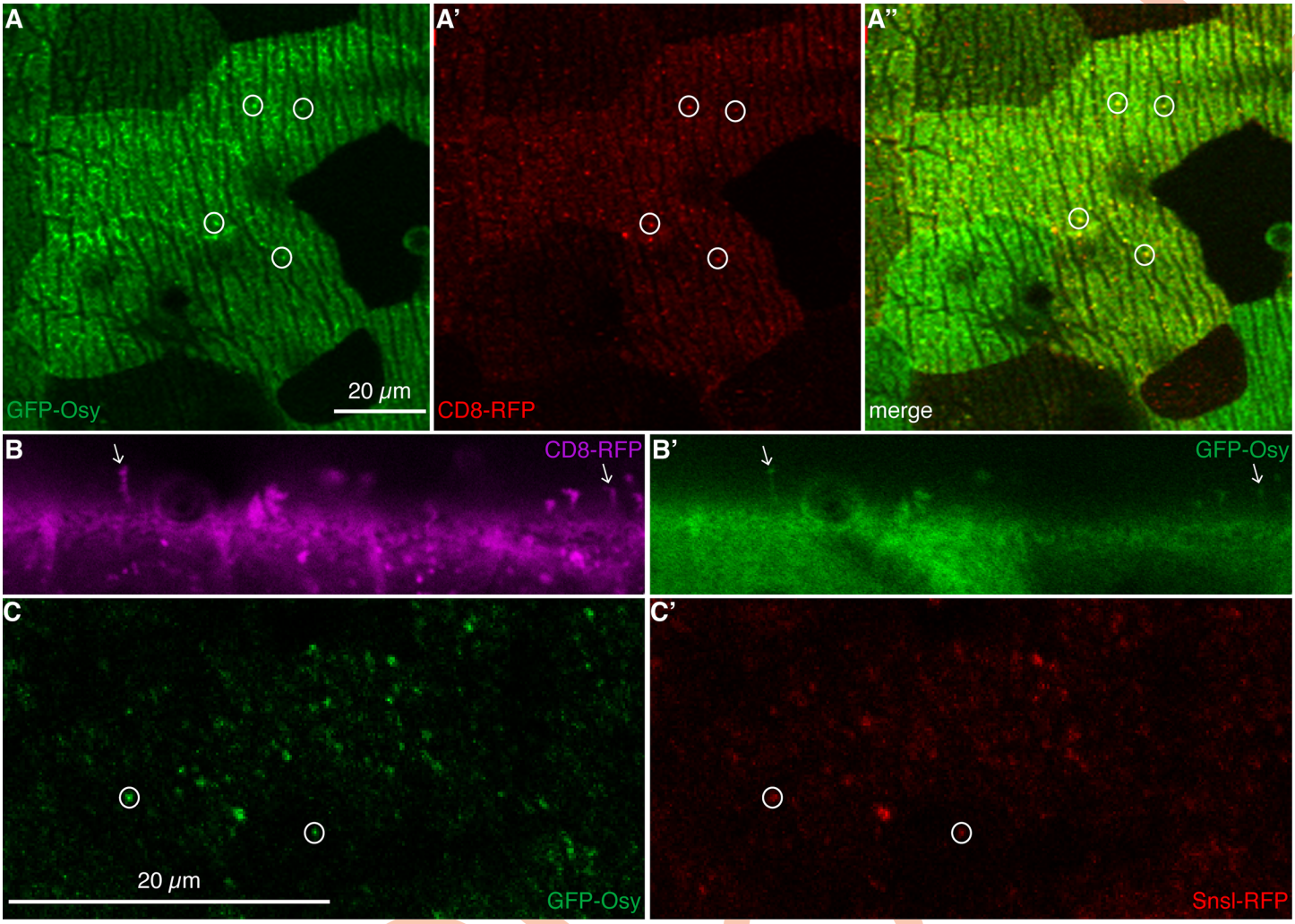

Fig 4. GFP-Osy localizes to pore canals. By confocal microscopy, in live L3 larvae, GFP-Osy (green) is detected at the surface of epidermal cells marked by ridges in the top view (A). As described recently, these ridges are produced by the basal site of the cuticle engraved into the apical plasma membrane of epidermal cells of L3 larvae [38]. Occasionally, the GFP signal accumulates forming dots (circles). These dots co-localise (yellow) with red membrane-marking CD8-RFP dots (A',A"). We observed that not all CD8-RFP dots coincided with a GFP-Osy signal; we suspect that there may be different CD8-RFP populations. Optical cross-sections confirm that CD8-RFP signals (magenta, B) protruding from the cell surface of live third instar larvae and marking pore canals coincide (arrows) with GFP-Osy signals (green, B'). In optical sections parallel to the surface, below the surface of the cuticle, dots of GFP-Osy signal are detected (C) that largely overlap with the signal of Snsl-RFP that marks the tips of potential pore canals (C'). Please note that images were taken sequentially of live animals, a perfect match of signals is therefore not expected.

https://doi.org/10.1371/journal.pgen.1008363.g004

In patients suffering severe mutation in the ABCA12 coding gene, abnormal lamellar granules accumulate in keratinocytes (Akiyama 2005, Yanagi 2008). We examined epidermal cells of wild-type and *osy* mutant larvae by electron microscopy in order to figure out whether in *osy* mutant larvae, lipid vesicles may also accumulate in the cell (S7 Fig). We found electron-lucid inclusions probably lipid-rich vesicles (Butterworth 1991) in the epidermis of *osy* mutant larvae that were missing in wild-type control larvae. Hence, disruption of lipid delivery to the cuticle surface is accompanied by accumulation of intracellular lipids.

Discussion

ABC transporters play important roles in cell and tissue homeostasis by mediating the exchange of solutes and metabolites across membranes. Here we show that Osy, a half-type

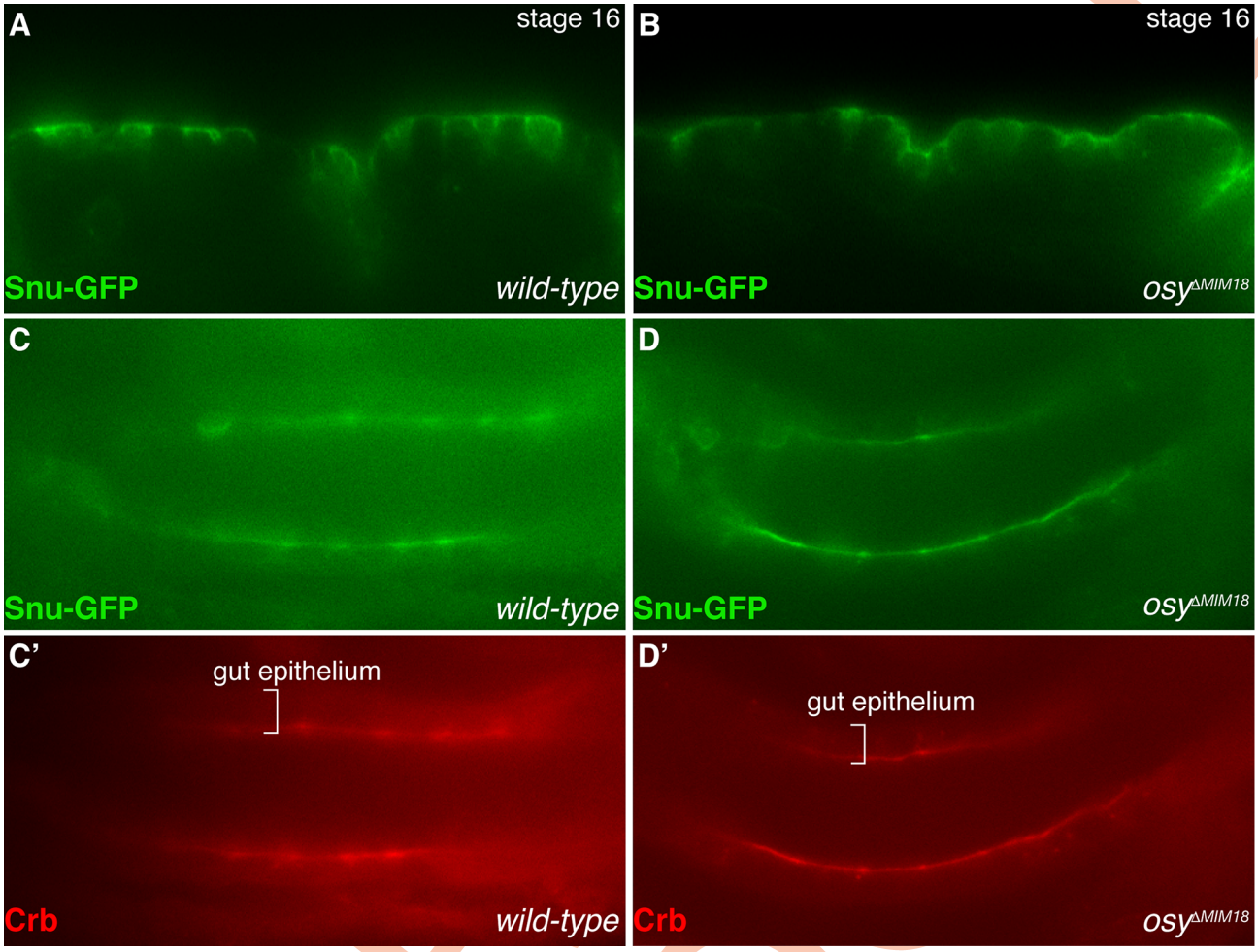

Fig 5. Localization of Snu does not depend on Osy. In stage 16 embryos, Snu-GFP (green) is recruited to the apical plasma membrane of epidermal and gut cells (A,C,C'). This localisation is independent of Osy function (B,D,D'). The apical plasma membrane of gut epithelial cells is marked with Crb (red, C',D'). A and B live embryos, C and D fixed embryos.

https://doi.org/10.1371/journal.pgen.1008363.g005

ABC transporter, is needed for transpiration as well as penetration control in *D. melanogaster*. Moreover, our data indicate that this transporter is directly or indirectly involved in the externalization of CHCs on the cuticular envelope of flies.

osy codes for a full and a truncated half-type ABC transporter version

The *osy* locus is predicted to have two transcription start sites resulting in three transcripts. Two alternative long mRNA transcribed from the same transcription start site encode the same protein, while a short mRNA starting with exon 7 of the locus encodes a truncated protein lacking the N-terminal NBD. By qPCR, we confirmed the presence of the long and a short *osy* transcripts in the developing embryo and the wing. No truncated version of the other two ABCH-type of transporters, Snu and CG11147, has been predicted or reported. In the literature, however, there are a few reports on truncated ABC transporters in vertebrates. Besides the full length protein, for instance, there are three truncated forms of the human ABCA9 that lack either the C-terminal NBD or even 80% of the full-length protein [30]. Two alternative transcription start sites in the human *MRP9* locus lead to mRNAs that code for a full length

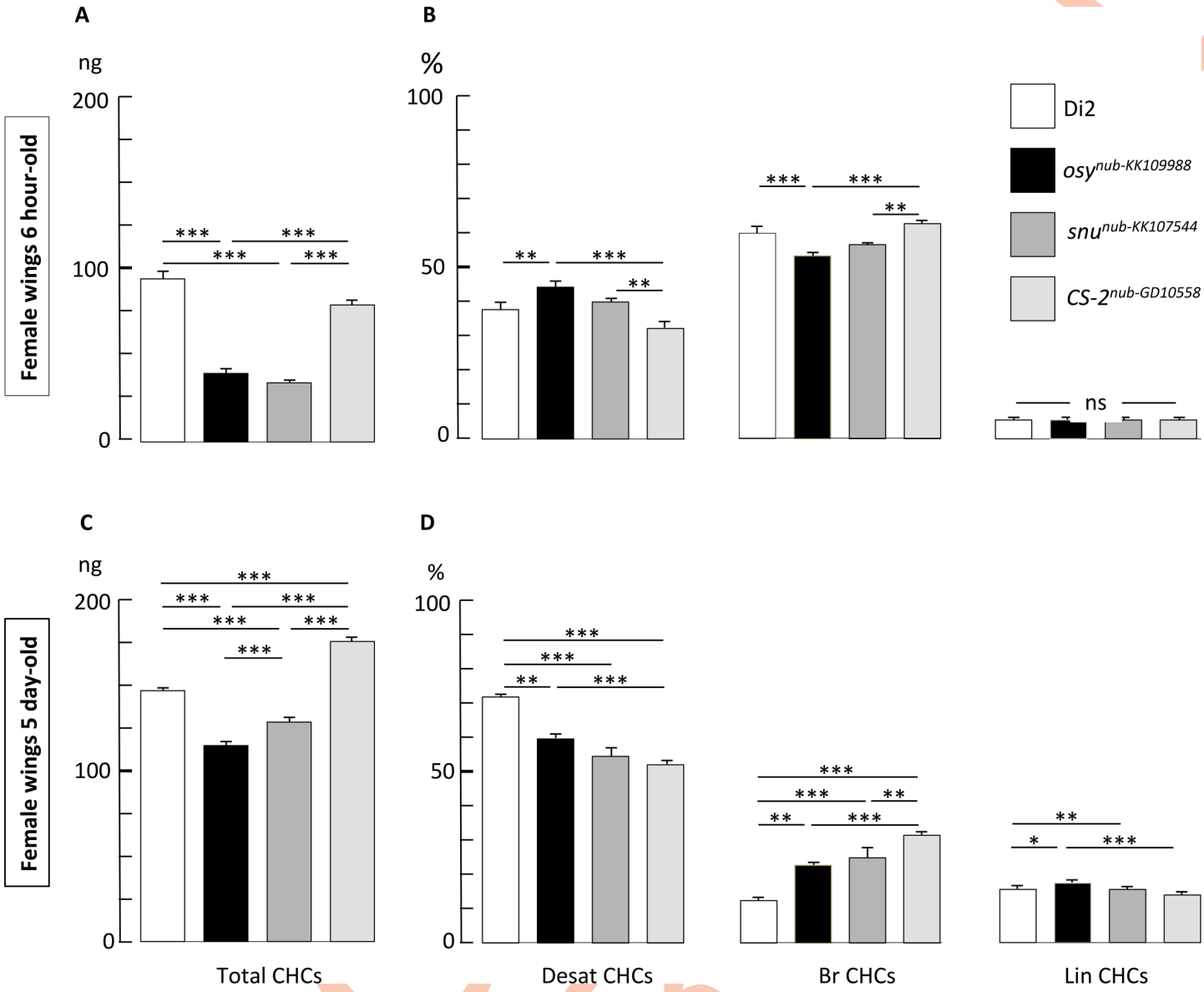

Fig 6. CHC amounts at the wing cuticle surface depend on Osy function. The principal groups of cuticular hydrocarbons (CHCs) measured in pair of wings of individual flies are shown in 6-hour-old (A, B) and 5-day old females (C, D). The genotypes tested are the wild-type Dijon2000 strain (empty bars), the progenies of *nub*-Gal4-RNAi crosses osy^{wgIR} (KK109988; bars with dark filling), snu^{wgIR} (bars with medium grey filling), and $CS\text{-}2^{wgIR}$ (bars with light grey filling). The graphs shown on the left (A, C) correspond to the mean (± sem) for the total absolute amount of CHs (Total CHCs) measured in ng. The graphs shown on the right (B, D) correspond to the relative level (%; calculated from the Total CHCs) for the sums of desaturated CHs (Desat CHCs), of branched CHCs (∑Br CHCs), and of linear saturated CHCs (Lin CHCs). Significant differences between genotypes were tested with a Kruskal Wallis test with Conover-Iman multiple pairwise comparisons -$\alpha = 0.05$, with Bonferroni correction; the level of significance between genotypes is indicated as: ***: $p<0.001$; **: $p<0.01$; *: $p<0.05$; ns: not significant. $N = 5$ for all genotypes and ages, except for 6 hour-old *snu* nub-KK107544 females: $N = 3$.

https://doi.org/10.1371/journal.pgen.1008363.g006

transporter or a truncated protein that harbours only the NBD, respectively [31]. In both cases, it is yet unknown whether the truncated proteins have any function. Taken together, our rescue experiments with a GFP-tagged full-length Osy version suggest that the putative truncated Osy protein translated from the short transcript is not essential, while the full-length protein version is needed for viability.

Insect ABCH transporters act in barrier construction or function

Insects have three ABCH-type transporters, ABCH-9A, -9B and -9C [18, 19]. In *D. melanogaster*, *T. castaneum* and *L. migratoria* ABCH-9C has been reported to be involved in the construction of the cuticle waterproof barrier [17–19]. In *D. melanogaster* and *L. migratoria*, it was shown that ABCH-9C is also needed to prevent xenobiotics penetration. In this work, we show that Osy, which represents the insect ABCH-9B in *D. melanogaster*, is required to prevent xenobiotics penetration into larvae and wings as well as desiccation in larvae. Thus, two ABCH-type transporters are implicated in the function of the cuticle outward and inward barrier in *D. melanogaster*. The third ABCH transporter CG11147 is expressed in the digestive system and is obviously not important for cuticle barrier function.

Osy and Snu act in parallel in barrier construction or function

The phenotype of *osy* mutant larvae is, compared to those provoked by mutations in *snu*, rather weak. The envelope structure of *snu* mutant larvae is reduced [17]. By consequence, the inward and outward barrier function of the cuticle is severely compromised. In contrast, the envelope structure appears to be normal in *osy* mutant larvae. Nevertheless, the inward and outward cuticle impermeability is also lost in these animals. Assuming that the bidirectional barrier function of the cuticle relies mainly on the integrity of the envelope, we speculate that Osy defines envelope quality without affecting envelope structure. Moreover, these findings indicate that Snu function in envelope construction is normal when Osy function is missing. Hence, Snu and Osy act in parallel in establishing the envelope-based barrier function of the *D. melanogaster* cuticle.

Osy is needed for CHC deposition on the surface of the cuticle

Previously, we had shown that Snu activity is needed for correct localisation of the extracellular protein Snsl to fine epidermal membrane protrusions that we propose to be pore canals [17]. Snsl, in turn, is needed for the apical distribution of envelope material that displays auto-florescence upon excitation with 405nm light. As pointed out above, these processes are unaffected in *osy* mutant larvae. Thus, Osy is not needed for Snsl trafficking and envelope formation. By contrast, CHC amounts are significantly reduced in wings with reduced *osy* expression. Additionally, we found that Osy-GFP localises to membrane protrusions within the cuticle and co-localizes with Snsl-RFP, reckoning that these structures represent pore canals. We therefore propose that the transporter activity of Osy is required for the amounts of CHC externalized and deposited on the surface of the cuticle via the pore canals. Whether Osy directly transports CHC to the cuticle surface or whether its function is needed indirectly for this process by establishing a structure that facilitates CHC transport remains to be investigated.

Analogies between vertebrate and invertebrate skin barrier formation

The establishment of a lipid-based ECM in the vertebrate skin involves the function of the ABC transporter ABCA12 [7, 32]. In humans, ABCA12 is involved in the deposition of lipids especially ceramides into lipid-transporting lamellar granules that subsequently release the lipid matrix into the intercellular space during differentiation of the stratum corneum [3, 6, 9]. Mutations in the ABCA12 coding gene cause depletion of lipids in the intercellular lipid layer ultimately provoking Harlequin-type ichthyosis (HI), lamellar ichthyosis type 2 (LI) or congenital ichthyosiform erythroderma (CIE), autosomal recessive congenital disorders associated with skin lesions that in severe cases may be fatal shortly after birth [3, 5]. Originally, ABCH transporters are possibly derived from ABCA transporters during evolution [25], and therefore

they may be lipid transporters, as well. Intriguingly, larvae with eliminated Osy function die shortly after hatching, and CHC levels are reduced in *osy* deficient wings, both paralleling humans with strong ABCA12 dysfunction. To some extent, hence, the molecular mechanisms of lipid deposition into the skin by an ABC transporter seem to be conserved between vertebrates and invertebrates. However, despite the deployment of similar molecular mechanisms, the subcellular mechanisms of lipid matrix formation i.e. the lipid delivery routes in *D. melanogaster* and vertebrates are fundamentally different. Neither are there any lamellar granules in the *D. melanogaster* embryonic or larval epidermal cells [33], nor are there any pore canals in the vertebrate corneocytes [34]. Thus, studies on Osy may contribute to our understanding of the molecular mechanisms of lipid barrier formation, but not to the underlying subcellular processes.

Materials and methods

Fly husbandry and genetics

Flies were cultivated in vials with standard cornmeal-based food at 18 or 25˚C. To collect embryos and larvae, flies were kept in cages on apple-juice plates garnished with fresh baker's yeast at 25˚C. Mutations were maintained over balancer chromosomes carrying insertions of GFP expressing marker genes (Dfd-YFP or Kr-GFP). This allowed us to identify homozygous non-GFP embryos or larvae as mutants under a fluorescence stereo-microscope (Leica). The line *twdlM-snsl-RFP* was described previously [17].

To generate genetically stable mutations in *osy*, the Minos elements in the coding sequence of $osy^{MB00606}$ were excised using heat-shock-induced *Minos*-transposase. Larvae and pupae were exposed to daily heat-shocks at 37˚C for 1 hour, thereby activating the *Minos*-transposase in the male germ line of the developing flies. Presence or absence of the *Minos* element was determined by the EGFP enhancer trap contained within the 7.5 kb element, which gives a fluorescent signal in the eyes of the flies. 19 Δ*Mi00606* stocks, all representing individual excision events, were established. The stocks were screened for viability of the homozygous Δ*Minos* allele. The primers used to amplify genomic DNA for sequencing of the excision footprint were CCATAGCACGCTCCAAATCA and TGCGCATCATCCACAAGAAG.

Sequence analyses

DNA and protein sequences were analysed using online software provided by NCBI conserved domain database and by the Expasy bioinformatics resource portal (expasy.org). Osy domain composition was predicted by the PSORT (http://www.psort.org), SignalP (http://www.cbs.dtu.dk/services/SignalP/) and by TMPred (https://embnet.vital-it.ch/software/TMPRED_form.html) software.

RNAi experiments

To down-regulate *osy* (*CG33970*) expression, the KK-line carrying the hairpin RNA construct with the ID 109988 or the GD-lines carrying the IDs 297 and 7619 constructs, respectively, were crossed to flies harbouring either *69B*-Gal4 (epidermis), BO-Gal4 (oenocytes) or both *da*-Gal4 and *7063*-Gal4 (ubiquitous and maternal Gal4, respectively). To down-regulate *osy* in wings, the KK-line was crossed to flies carrying *nub*-Gal4. As a control, the hairpin RNA construct directed against the midgut *chitin synthase 2* (*CS-2*) with the ID GD 10588 was used.

Construction of a GFP-tagged variant of Osy

Total mRNA was prepared from OregonR wild-type stage 17 embryos (RNeasy Micro Kit, Qiagen) and used to produce cDNA (Superscript III First-Strand Synthesis System,

Invitrogen). For amplification of both annotated isoforms of *osy* from this cDNA pool, two alternative 5' primers, ATGGACGCCGCTGCC and ATGCTGGCAGAGGAATCGC, as well as a single 3' primer, GCTGCTCAAGTTCAAGAAGGGATAA were used. The products were directly ligated into the pCR8/GW/TOPO vector. Sequencing of the purified vector DNA (Miniprep kit, Qiagen) confirmed the presence of *osy* coding isoforms A/B and C. Next, LR recombination was used to clone these sequences into Gateway vector pTGW, which contains a UAS promoter and a *GFP* tag 5' to the insert. The vector containing *osy* isoform C failed to amplify in bacteria and was rejected. The vector with the A/B isoforms was amplified in DH5α *E. coli* bacteria, purified (PerfectPrep Endofree Maxi Kit, 5Prime) and sent to Fly-Facility (Clermont-Ferrand, France) for transformation of *D. melanogaster* embryos.

Quantitative RT-PCR

Total mRNA was isolated from OregonR or Dijon2000 wild-type stage 17 embryos (RNeasy Micro Kit, Qiagen), and total cDNA was prepared (Superscript III First-Strand Synthesis System, Invitrogen). For each embryo collection, at least two independent RNA extractions were assayed three times in parallel. RT-PCR was performed with an iCycler and iTaq SYBR Green Supermix, Biorad. The primers used were GCAATATGTGACCGACGATG and GCGGTA CAGCAACTGTGAGA, which amplify a 208 bp fragment common to all *osy* isoforms. The primers TGAGTGACAAAACAGGGATCTT and CGATTCCTCTGCCAGCATTT were used to amplify the short *osy* isoform. As a reference, the primers CGTCGAGGCGGTGTGAAGC and TTAACCGCCAAATCCGTAGAGG that amplify a 195 bp fragment of *histone H4* were used. REST software was used to determine the crossing point differences (DCP value) of individual transcripts in treated (sample) and non-treated (control) embryos [35]. The efficiency (*E*) corrected relative expression ratio of the target gene was calculated using the DCP value of *histone H4* expression according to the equation

$$\text{Ratio} = E\,(\text{target})^{\Delta CP\ \text{target}\ (\text{control}-\text{sample})} / E\,(\text{reference})^{\Delta CP\ \text{reference}\ (\text{control}-\text{sample})}$$

A two-fold change in gene expression was defined as the cut-off for acceptance, as changes up to two-fold are observed also when different wild-type samples are compared [36].

Microscopy

For transmission electron microscopy (TEM), embryos and larvae were treated and analysed on a Philips CM-10 electron microscope as described in detail previously [37]. Bright field, differential interference contrast (DIC) and fluorescence microscopy were performed with a Nikon eclipse E1000 or a Zeiss Axioplan 2 microscope. Confocal imaging was performed with Zeiss LSM 710 Axio Observer or LSM 800, Bio-Rad Radiance 2000 or Leica TCS SP2. Figures were prepared using the Adobe Photoshop CS6 and Adobe Illustrator CS6 software.

Chemical analysis of CHCs

To extract cuticular hydrocarbons, 6-hour or 5-day old flies were frozen for 5 min at -20˚C just before removing the wings using micro-scissors. Each pair of wings was immersed for 10 min at room temperature into vials containing 20 μL of hexane. The solution also contained 3.33 ng/μl of C26 (*n*-hexacosane) and 3.33 ng/μl of C30 (*n*-triacontane) as internal standards. After removing the wings, the extracts were stored at -20˚C until analysis. All extracts were analyzed using a Varian CP3380 gas chromatograph fitted with a flame ionization detector, a CP Sil 5CB column (25 m × 0.25 mm internal diameter; 0.1 μm film thickness; Agilent), and a split–splitless injector (60 ml/min split-flow; valve opening 30 s after injection) with helium as

carrier gas (velocity = 50 cm/s at 120˚C). The temperature program began at 120˚C, ramping at 10˚C/min to 140˚C, then ramping at two˚C/min to 290˚C, and holding for 10 min. The chemical identity of the cuticular hydrocarbons was checked using gas chromatography-mass spectrometry system equipped with a CP Sil 5CB column (Everaerts et al., 2010). The amount (ng/insect) of each component was calculated based on the readings obtained from the internal standards. For the sake of clarity we only show the principal CH groups: the overall CHs sum (ΣCHs), the sum of desaturated CHs (ΣDesat), the sum of linear saturated CHs (ΣLin) and the sum of branched CHs (ΣBranched).

Supporting information

S1 Fig. Represented by protein sequences from the hemimetabolous insect *Locusta migratoria* and the holometabolous insect *D. melanogaster*, insect species have three H-type ABC transporters. The ancestral protein that is shared with crustaceans (*Daphnia*), is ABCH-9A (CG11147 in *D. melanogaster*).
(TIF)

S2 Fig. As analysed by qPCR, expression of *osy* hpRNA (KK-109988) in the oenocytes driven by BO-Gal4 does not reduce larval *osy* transcript levels compared to the transcript levels in control larvae (Oregon). The progeny of this cross was viable to adulthood. Three independent experiments were conducted. For qPCR analyses, two technical replicates per experiment were performed.
(TIF)

S3 Fig. Freshly hatched wild-type larvae (control) have a spindle-like body shape. Often they are immobile before they start crawling to a food source. Larvae with eliminated *osy* function ($osy^{\Delta MiM18}$) at around 15 minutes after hatching stop moving and start flattening. See also supplementary movies 1 and 2.
(TIFF)

S4 Fig. Osy-GFP expressed in the epidermis (*69B*-Gal4, UAS-*osyGFP*) or ubiquitously (tub-Gal4, UAS-*osyGFP*) normalises the cuticle impermeability in $osy^{\Delta MiM18}$ homozygous mutant larvae (compare to Fig 3).
(TIF)

S5 Fig. Wings of control flies expressing hpRNA against midgut chitin synthase 2 transcripts (*nub*-Gal4 x UAS-*CS-2*^{wgIR}, *CS-2*^{wgIR}) are impermeable to Eosin Y until 50˚C. At 55˚C, the dye penetrates the posterior margin of the wing of these flies. Penetration is more pronounced at higher temperatures (60˚C). Wings of flies expressing hpRNA against *osy* (*nub*-Gal4 x UAS-*KK109988*, osy^{wgIR}) transcripts are impermeable to Eosin Y until 45˚C. Eosin Y penetrates the posterior half of the wing of these flies at 50˚C, and the whole wing at 55˚C. It should be noted that osy^{wgIR} wings did not show any obvious morphological defect and the respective flies survived and did not desiccate.
(TIF)

S6 Fig. A detailed list of the CHCs analysed and summarised in Fig 6.
(TIFF)

S7 Fig. Electron-micrographs of the epidermis of wild-type (A) and $osy^{\Delta MiM18}$ first instar larvae (B). Electron-lucid round structures (triangles) probably representing lipid droplet-like organelles were found in the $osy^{\Delta MiM18}$ epidermal cells. These structures were missing in the wild-type control epidermis. Due to preparation of the specimens with acetone, lipids are

usually extracted from the probes. Therefore, these structures are electron-lucid and appear to be empty.
(TIF)

S1 Movie. On an agar plate, freshly hatched osy$^{\Delta MiM18}$ larvae die soon after hatching and flatten. For filming, eggs of an over-night egg lay were dechorionated with 50% bleach for 3 minutes in a mesh basket. They were transferred with a soft brush to a fresh agar plate and allowed to fully develop to larvae. This experiment was repeated three times, each with more than 10 larvae.
(MOV)

S2 Movie. On an agar plate, freshly hatched *osy$^{\Delta MiM18}$* larvae submerged in halocarbon oil survive more than 120 minutes (see Table 1). The movie was stopped here after 100 minutes. Eggs and larvae were handled as for S1 Movie.
(MOV)

Acknowledgments

We thank Sven Hülsmann for assistance with confocal microscopy.

Author Contributions

Conceptualization: Michaela Norum, Bernard Moussian.

Data curation: Bernard Moussian.

Formal analysis: Yiwen Wang, Michaela Norum, Kathrin Oehl, Renata Zuber, Jean-Pierre Farine, Nicole Gehring, Matthias Flötenmeyer, Jean-François Ferveur, Bernard Moussian.

Funding acquisition: Bernard Moussian.

Investigation: Yiwen Wang, Michaela Norum, Kathrin Oehl, Yang Yang, Renata Zuber, Jing Yang, Jean-Pierre Farine, Matthias Flötenmeyer, Jean-François Ferveur, Bernard Moussian.

Methodology: Yiwen Wang, Michaela Norum, Jean-François Ferveur, Bernard Moussian.

Project administration: Bernard Moussian.

Resources: Bernard Moussian.

Software: Bernard Moussian.

Supervision: Bernard Moussian.

Validation: Bernard Moussian.

Visualization: Bernard Moussian.

Writing – original draft: Michaela Norum, Bernard Moussian.

Writing – review & editing: Bernard Moussian.

References

1. Rabionet M, Gorgas K, Sandhoff R. Ceramide synthesis in the epidermis. Biochim Biophys Acta. 2014; 1841(3):422–34. https://doi.org/10.1016/j.bbalip.2013.08.011 PMID: 23988654.
2. Zaki T, Choate K. Recent advances in understanding inherited disorders of keratinization. F1000Res. 2018;7. https://doi.org/10.12688/f1000research.13350.2 PMID: 30002814; PubMed Central PMCID: PMC6024232.

3. Akiyama M. Corneocyte lipid envelope (CLE), the key structure for skin barrier function and ichthyosis pathogenesis. J Dermatol Sci. 2017; 88(1):3–9. https://doi.org/10.1016/j.jdermsci.2017.06.002 PMID: 28623042.
4. Akiyama M. The roles of ABCA12 in keratinocyte differentiation and lipid barrier formation in the epidermis. Dermato-endocrinology. 2011; 3(2):107–12. https://doi.org/10.4161/derm.3.2.15136 PMID: 21695020; PubMed Central PMCID: PMC3117010.
5. Akiyama M. The roles of ABCA12 in epidermal lipid barrier formation and keratinocyte differentiation. Biochim Biophys Acta. 2014; 1841(3):435–40. https://doi.org/10.1016/j.bbalip.2013.08.009 PMID: 23954554.
6. Akiyama M, Sugiyama-Nakagiri Y, Sakai K, McMillan JR, Goto M, Arita K, et al. Mutations in lipid transporter ABCA12 in harlequin ichthyosis and functional recovery by corrective gene transfer. J Clin Invest. 2005; 115(7):1777–84. https://doi.org/10.1172/JCI24834 PMID: 16007253; PubMed Central PMCID: PMC1159149.
7. Kelsell DP, Norgett EE, Unsworth H, Teh MT, Cullup T, Mein CA, et al. Mutations in ABCA12 underlie the severe congenital skin disease harlequin ichthyosis. Am J Hum Genet. 2005; 76(5):794–803. https://doi.org/10.1086/429844 PMID: 15756637; PubMed Central PMCID: PMC1199369.
8. Rajpar SF, Cullup T, Kelsell DP, Moss C. A novel ABCA12 mutation underlying a case of Harlequin ichthyosis. Br J Dermatol. 2006; 155(1):204–6. https://doi.org/10.1111/j.1365-2133.2006.07291.x PMID: 16792777.
9. Scott CA, Rajpopat S, Di WL. Harlequin ichthyosis: ABCA12 mutations underlie defective lipid transport, reduced protease regulation and skin-barrier dysfunction. Cell Tissue Res. 2013; 351(2):281–8. https://doi.org/10.1007/s00441-012-1474-9 PMID: 22864982.
10. Thomas AC, Cullup T, Norgett EE, Hill T, Barton S, Dale BA, et al. ABCA12 is the major harlequin ichthyosis gene. J Invest Dermatol. 2006; 126(11):2408–13. https://doi.org/10.1038/sj.jid.5700455 PMID: 16902423.
11. Moussian B. Recent advances in understanding mechanisms of insect cuticle differentiation. Insect Biochem Mol Biol. 2010; 40(5):363–75. Epub 2010/03/30. S0965-1748(10)00070-6 [pii] https://doi.org/10.1016/j.ibmb.2010.03.003 PMID: 20347980.
12. Blomquist GJ, Bagneres AG. Insect Hydrocarbons: Biology, Biochemistry, and Chemical Ecology: Cambridge University Press; 2010.
13. Gutierrez E, Wiggins D, Fielding B, Gould AP. Specialized hepatocyte-like cells regulate Drosophila lipid metabolism. Nature. 2007; 445(7125):275–80. Epub 2006/12/01. nature05382 [pii] https://doi.org/10.1038/nature05382 PMID: 17136098.
14. Ferveur JF. The pheromonal role of cuticular hydrocarbons in Drosophila melanogaster. Bioessays. 1997; 19(4):353–8. Epub 1997/04/01. https://doi.org/10.1002/bies.950190413 PMID: 9136633.
15. Wicker-Thomas C, Garrido D, Bontonou G, Napal L, Mazuras N, Denis B, et al. Flexible origin of hydrocarbon/pheromone precursors in Drosophila melanogaster. J Lipid Res. 2015; 56(11):2094–101. https://doi.org/10.1194/jlr.M060368 PMID: 26353752; PubMed Central PMCID: PMC4617396.
16. Qiu Y, Tittiger C, Wicker-Thomas C, Le Goff G, Young S, Wajnberg E, et al. An insect-specific P450 oxidative decarbonylase for cuticular hydrocarbon biosynthesis. Proc Natl Acad Sci U S A. 2012; 109 (37):14858–63. https://doi.org/10.1073/pnas.1208650109 PMID: 22927409; PubMed Central PMCID: PMC3443174.
17. Zuber R, Norum M, Wang Y, Oehl K, Gehring N, Accardi D, et al. The ABC transporter Snu and the extracellular protein Snsl cooperate in the formation of the lipid-based inward and outward barrier in the skin of Drosophila. Eur J Cell Biol. 2018; 97(2):90–101. https://doi.org/10.1016/j.ejcb.2017.12.003 PMID: 29306642.
18. Yu Z, Wang Y, Zhao X, Liu X, Ma E, Moussian B, et al. The ABC transporter ABCH-9C is needed for cuticle barrier construction in Locusta migratoria. Insect Biochem Mol Biol. 2017; 87:90–9. https://doi.org/10.1016/j.ibmb.2017.06.005 PMID: 28610908.
19. Broehan G, Kroeger T, Lorenzen M, Merzendorfer H. Functional analysis of the ATP-binding cassette (ABC) transporter gene family of Tribolium castaneum. BMC Genomics. 2013; 14:6. https://doi.org/10.1186/1471-2164-14-6 PMID: 23324493; PubMed Central PMCID: PMC3560195.
20. Liu S, Zhou S, Tian L, Guo E, Luan Y, Zhang J, et al. Genome-wide identification and characterization of ATP-binding cassette transporters in the silkworm, Bombyx mori. BMC Genomics. 2011; 12:491. https://doi.org/10.1186/1471-2164-12-491 PMID: 21981826; PubMed Central PMCID: PMC3224256.
21. Bretschneider A, Heckel DG, Vogel H. Know your ABCs: Characterization and gene expression dynamics of ABC transporters in the polyphagous herbivore Helicoverpa armigera. Insect Biochem Mol Biol. 2016; 72:1–9. https://doi.org/10.1016/j.ibmb.2016.03.001 PMID: 26951878.

22. Pignatelli P, Ingham VA, Balabanidou V, Vontas J, Lycett G, Ranson H. The Anopheles gambiae ATP-binding cassette transporter family: phylogenetic analysis and tissue localization provide clues on function and role in insecticide resistance. Insect Mol Biol. 2018; 27(1):110–22. https://doi.org/10.1111/imb.12351 PMID: 29068552.

23. Qi W, Ma X, He W, Chen W, Zou M, Gurr GM, et al. Characterization and expression profiling of ATP-binding cassette transporter genes in the diamondback moth, Plutella xylostella (L.). BMC Genomics. 2016; 17(1):760. https://doi.org/10.1186/s12864-016-3096-1 PMID: 27678067; PubMed Central PMCID: PMC5039799.

24. Dermauw W, Osborne EJ, Clark RM, Grbic M, Tirry L, Van Leeuwen T. A burst of ABC genes in the genome of the polyphagous spider mite Tetranychus urticae. BMC Genomics. 2013; 14:317. https://doi.org/10.1186/1471-2164-14-317 PMID: 23663308; PubMed Central PMCID: PMC3724490.

25. Dermauw W, Van Leeuwen T. The ABC gene family in arthropods: comparative genomics and role in insecticide transport and resistance. Insect Biochem Mol Biol. 2014; 45:89–110. https://doi.org/10.1016/j.ibmb.2013.11.001 PMID: 24291285.

26. Pasello M, Giudice AM, Scotlandi K. The ABC subfamily A transporters: multifaceted players with incipient potentialities in cancer. Semin Cancer Biol. 2019. https://doi.org/10.1016/j.semcancer.2019.10.004 PMID: 31605751.

27. Wang Y, Carballo RG, Moussian B. Double cuticle barrier in two global pests, the whitefly Trialeurodes vaporariorum and the bedbug Cimex lectularius. J Exp Biol. 2017;220(Pt 8):1396–9. https://doi.org/10.1242/jeb.156679 PMID: 28167802.

28. Wang Y, Yu Z, Zhang J, Moussian B. Regionalization of surface lipids in insects. Proc Biol Sci. 2016;283(1830). https://doi.org/10.1098/rspb.2015.2994 PMID: 27170708; PubMed Central PMCID: PMC4874700.

29. Teasdale RD, Jackson MR. Signal-mediated sorting of membrane proteins between the endoplasmic reticulum and the golgi apparatus. Annu Rev Cell Dev Biol. 1996; 12:27–54. https://doi.org/10.1146/annurev.cellbio.12.1.27 PMID: 8970721.

30. Piehler A, Kaminski WE, Wenzel JJ, Langmann T, Schmitz G. Molecular structure of a novel cholesterol-responsive A subclass ABC transporter, ABCA9. Biochem Biophys Res Commun. 2002; 295 (2):408–16. Epub 2002/08/02. https://doi.org/10.1016/s0006-291x(02)00659-9 PMID: 12150964.

31. Bera TK, Iavarone C, Kumar V, Lee S, Lee B, Pastan I. MRP9, an unusual truncated member of the ABC transporter superfamily, is highly expressed in breast cancer. Proc Natl Acad Sci U S A. 2002; 99 (10):6997–7002. Epub 2002/05/16. https://doi.org/10.1073/pnas.102187299 PMID: 12011458; PubMed Central PMCID: PMC124517.

32. Li Q, Frank M, Akiyama M, Shimizu H, Ho SY, Thisse C, et al. Abca12-mediated lipid transport and Snap29-dependent trafficking of lamellar granules are crucial for epidermal morphogenesis in a zebrafish model of ichthyosis. Dis Model Mech. 2011; 4(6):777–85. https://doi.org/10.1242/dmm.007146 PMID: 21816950; PubMed Central PMCID: PMC3209647.

33. Moussian B, Seifarth C, Muller U, Berger J, Schwarz H. Cuticle differentiation during Drosophila embryogenesis. Arthropod Struct Dev. 2006; 35(3):137–52. Epub 2007/12/20. S1467-8039(06)00020-X [pii] https://doi.org/10.1016/j.asd.2006.05.003 PMID: 18089066.

34. Yanagi T, Akiyama M, Nishihara H, Sakai K, Nishie W, Tanaka S, et al. Harlequin ichthyosis model mouse reveals alveolar collapse and severe fetal skin barrier defects. Hum Mol Genet. 2008; 17 (19):3075–83. https://doi.org/10.1093/hmg/ddn204 PMID: 18632686.

35. Pfaffl MW, Horgan GW, Dempfle L. Relative expression software tool (REST) for group-wise comparison and statistical analysis of relative expression results in real-time PCR. Nucleic Acids Res. 2002; 30 (9):e36. Epub 2002/04/25. https://doi.org/10.1093/nar/30.9.e36 PMID: 11972351; PubMed Central PMCID: PMC113859.

36. Gangishetti U, Breitenbach S, Zander M, Saheb SK, Muller U, Schwarz H, et al. Effects of benzoylphenylurea on chitin synthesis and orientation in the cuticle of the Drosophila larva. Eur J Cell Biol. 2009; 88 (3):167–80. Epub 2008/11/11. S0171-9335(08)00134-9 [pii] https://doi.org/10.1016/j.ejcb.2008.09.002 PMID: 18996617.

37. Moussian B, Schwarz H. Preservation of plasma membrane ultrastructure in Drosophila embryos and larvae prepared by high-pressure freezing and freeze-substitution. Drosophila Information Service. 2010; 93:215–9.

38. Tajiri R, Ogawa N, Fujiwara H, Kojima T. Mechanical Control of Whole Body Shape by a Single Cuticular Protein Obstructor-E in Drosophila melanogaster. PLoS Genet. 2017; 13(1):e1006548. https://doi.org/10.1371/journal.pgen.1006548 PMID: 28076349; PubMed Central PMCID: PMC5226733.